N94-14663

Rain Rate Duration Statistics Derived from the Mid-Atlantic Coast Rain Gauge Network

Julius Goldhirsh
The Johns Hopkins University, Applied Physics Laboratory
Johns Hopkins Road, Laurel Maryland, 20723-6099

Abstract

A rain gauge network comprised of 10 tipping bucket rain gauges located in the Mid-Atlantic coast of the United States has been in continuous operation since June 1, 1986. Rain rate distributions and estimated slant path fade distributions at 20 GHz and 30 GHz covering the first five year period have been derived from the gauge network measurements, and these results have been described by Goldhirsh et al. [1]. In this effort, we present rain rate *time duration* statistics. The rain duration statistics are of interest for better understanding the physical nature of precipitation and to present a data base which may be used by modelers to convert to slant path fade duration statistics. Such statistics are important for better assessing optimal coding procedures over defined bandwidths.

1.0 Review of Experimental Configuration

The rain gauges are of the tipping bucket type described by Goldhirsh and Gebo [2] and Gebo and Goldhirsh [3]. Each rain gauge is interfaced with an individual PC which records the tipping times from which the rain rates are derived. The gauges are located within a rectangular grid whose north-south and east-west distances are 70 km and 47 km, respectively. The gauge locations are shown on the map of Figure 1 and are numbered from 1 to 10. Calibrations are performed twice per year and the system is maintained with errors of less than 5% in rainfall at rates of 12 to 15 mm/h.

2.0 Review of Rain Rate Distributions

For purpose of completeness, we review the previously reported pertinent cumulative fade distributions. In Figure 2 are given the individual network average rain rate distributions for years 1 through 5, where year 1 covered the period 1 June 1986–31 May 1987, and subsequent year numbers covered the respective contiguous 12 month periods. Site #6 operated during the first three years and Site #4 operated during the latter four year period. These intervals were accounted for in determining the resultant network and yearly averages. We note years 1, 2, 3, and 5 show similar distributions, whereas year 4 shows significantly higher probabilities. The combined distribution, which is the spatial and temporal average, is given by the circled points and represents the equivalent of 47 site-years of measurements. This set of distributions indicates that it took four years before an extreme rain rate distribution was noted. As of this writing, approximately seven years of network data have been accumulated, and it is the intent to reexamine the annual variability after 10 years of network data are available. Figure 3 shows distributions for each of the 10 sites, where each corresponds to the five year temporal average (with the exception of Sites #4 and #6). The combined spatial and temporal average is given by the distribution with the circled points. We note the spatial variability of the distributions (Figure 3) is significantly smaller than the temporal variability (Figure 2).

3.0 Rain Rate Durations

3.1 Methodology of Formulation

Consistent with the definition of Vogel et al. [4], a rain rate *episode* represents the continuous time interval a designated rain rate threshold level is exceeded. The conditional probability of exceeding a rain rate duration for a given rain episode level is defined as follows

$$P(D > D_q | R > R_q) = \frac{N(D > D_q | R > R_q)}{N_T(R > R_q)} \tag{1}$$

where

R	Rain rate in mm/h
R_q	Designated threshold rain rate value or episode threshold
D	Duration of rain rate episode
D_q	Designated threshold duration pertaining to rain rate episode level
$N(D > D_q \vert R > R_q)$	Number of episodes for which $D > D_q$ given $R > R_q$
$N_T(R > R_q)$	Total number of episodes for which $R > R_q$

Cumulative probability distributions of the type given by (1) were obtained from density distributions containing 150 contiguous duration bins whose bin size was one minute.

3.2 Temporal and Spatial Average

In Figure 4 are given a family of distributions pertaining to a temporal and spatial average of the rain rate site data for rain rate thresholds of 5, 10, 20, 50, 100, and 125 mm/h. We note that for any given probability the rain rate durations decrease with increasing rain rate, and conversely. This characteristic is amplified in Figure 5 where the duration is plotted versus rain rate for fixed probability levels (solid levels). The curves follow an approximate power law curve in the range 5 mm/h to 50 mm/h, and thereafter the durations tend to fall off more rapidly with increasing rain rate. By expressing each curve by it's best fit power curve (for the indicated range of rain rates), we obtain

$$D = A(P)\, R^{-B(P)} \qquad 5 \le R \le 50 \tag{2}$$

where D is the rain rate duration in minutes and R is the rain rate in mm/h. A family of A and B values were derived for each percentage level and best fit functional forms were determined which fit the A versus P and B versus P relations [5]. The functions are given by

$$A(P) = \left(a + b\, P^{0.5}\, \ln P\right)^{-1} \tag{3}$$

$$B(P) = c + d\, \exp(P/e) \tag{4}$$

where

$$\begin{cases} a = 3.28322 \times 10^{-3} \\ b = 9.17138 \times 10^{-4} \\ c = 9.31395 \times 10^{-1} \\ d = 1.16276 \times 10^{-2} \\ e = 2.31520 \times 10^{1} \end{cases} \tag{5}$$

where P is the probability of exceeding the duration D and is expressed in percent. The resultant set of empirically derived fits are given by the dashed curves in Figure 6. We note that the expression (2) fits the measured levels very well for all probabilities indicated. The difference between the measured and empirically derived durations at 50 mm/h for the 50% case is less than 0.3 min. The overall average of the absolute differences between the measured durations and empirically derived durations is 0.5 min with the RMS being 1.3 min for the system of curves.

3.3 Site-to-Site Variability

In Figure 7 we compare the site-to-site variability of the rain duration distributions for the 10 sites for the different rain rate thresholds, where each site is averaged over the five year period. The peak spread was determined for a series of fixed probabilities in Figure 7 and the resultant equi-probability values versus distribution spread is plotted in Figure 8 for the series of rain rate thresholds. The curve for the threshold value of 100 mm/h, which not shown in Figure 7, is also plotted in Figure 8.

We glean the following characteristics from Figures 7 and 8: [1] The distributions are grouped into bundles associated with the indicated rain rate threshold (Figure 7). [2] The spread of distributions (for any given rain rate threshold), increases monotonically with increasing rain rate duration (Figure 7). [3] The distribution spread increases monotonically with decreasing rain rate threshold (Figure 8).

The narrowness of the distribution spread for probabilities above 10% is indicative of the fact that the spatial structure of the rain cells and its dynamics are similar statistically for each rain rate threshold over the lateral scale dimensions defining the separations of the ten sites.

3.4 Year-Year Variability

In Figure 9 is plotted a family of curves representing the network average distribution for each year of the five year period. The resultant set of curves is a manifestation of the year to year variability of the rain rate durations. In Figure 10 are plotted the corresponding equi-probability values versus the distribution spread for the family of rain rate thresholds considered. The characteristics are similar to those described in the previous section. The narrowness of the distribution spread for probabilities greater than 10% is indicative of the fact that the spatial structure of the rain cells and its dynamics are statistically similar for any given rain rate threshold from year to year. What differs from year to year is the frequency of occurrence of the rain rate threshold. However, once the rain events occur, the conditional statistics are relatively invariant.

4.0 Comparison with Other Investigators

We compare here the rain rate duration distributions examined here with those recently published for Austin, Texas over the four year period from June 1988–May 1992 [4]. Figure 11 presents a comparison of the cumulative rain rate distributions of Austin, Texas and the Mid-Atlantic coast combined average case, and Figure 12 shows the corresponding rain duration distributions. We note that although the rain rate distributions are considerably different (Figure 11), the rain duration distributions are remarkable similar (Figure 12); especially at probabilities greater than 10% for all rain rate thresholds. Excellent agreement is noted for probabilities of 1% and greater for rain rate thresholds larger than 10 mm/h. The equal probability differences are well within the spread durations for the individual sites denoted in Figure 8. The proximity of the duration distributions indicate that for the two regions, the statistics associated with the structure and dynamics of rain cells are relatively invariant, although the absolute probability of occurrence varies.

5.0 Summary and Conclusions

Rain rate time durations were analyzed employing a data base covering the first five years of measurements from the Mid-Atlantic coast tipping bucket rain gauge network comprised of 10 gauges. An empirical rain rate model was developed which characterizes the combined network average (temporal and spatial) of the probability of time duration of rain rate episodes to within an overall average error of 0.5 minutes (equation (2)). The narrowness of the spread of distributions for the year-to-year and site-to-site cases are indicative that given a rain rate threshold, the duration statistics are relatively invariant. A comparison of the the Mid-Atlantic coast rain rate duration distributions with those from Austin, Texas showed close agreement. The above results demonstrate that although the frequency of occurrence of a rain rate threshold may vary from year to year and location to location, once the threshold is exceeded, the dynamics and rain cell structures are generally statistically invariant.

6.0 Acknowledgements

The author is grateful to Norman Gebo who manages the rain gauge network and to Vladimir Krichevsky who developed the rain duration software and reduced the five year data set. This work was supported by the NASA Propagation Program directed by the Office of Commercial Programs under Contract NOO39-91-C-001.

7.0 References

1 Goldhirsh, J. V. Krichevsky, and N. E. Gebo, "Rain Rate Statistics and Fade Distributions at 20 and 30 GHz Derived from a Network of Rain Gauges in the Mid-Atlantic Coast over a Five Year Period," *IEEE Trans. Ant. & Prop.*, Vol. 40, No. 11, pp. 1408–1415, November, 1992.

2 Goldhirsh, J. and N. E. Gebo, "A Comparative Assessment of R. M. Young and Tipping Bucket Rain Gauges," *JHU/APL Technical Report S1R-92U-018*, June 1992.

3 Gebo, N. E. and J. Goldhirsh, "Operation, Calibration, and Data Acquisition for Capacitive and Tipping Bucket Rain Gauges," *JHU/APL Technical Report S1R93U-004*, March 1993.

4 Vogel et al., "Rain Fades on Low Elevation Angle Earth-Satellite Paths: Comparative Assessment of the Austin, Texas 11.2 GHz Experiment," *Proceedings of the IEEE*, June, 1993.

5 Jandel Scientific, "TableCurve, Automated Curve Fitting Software," Jandel Scientific, San Rafael, CA 94901.

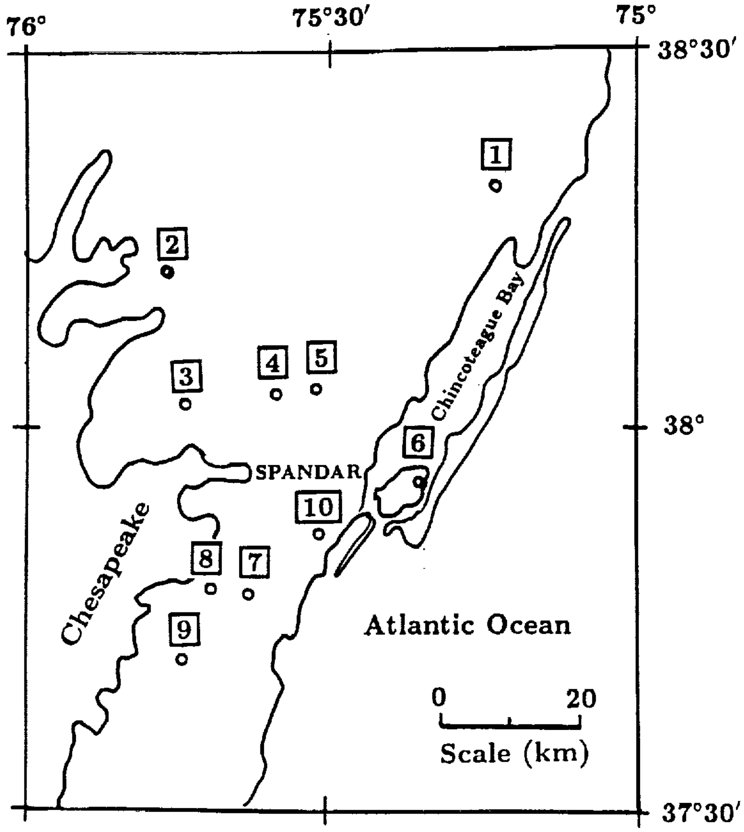

Figure 1: Map of Mid-Atlantic coast region designating rain gauge site locations.

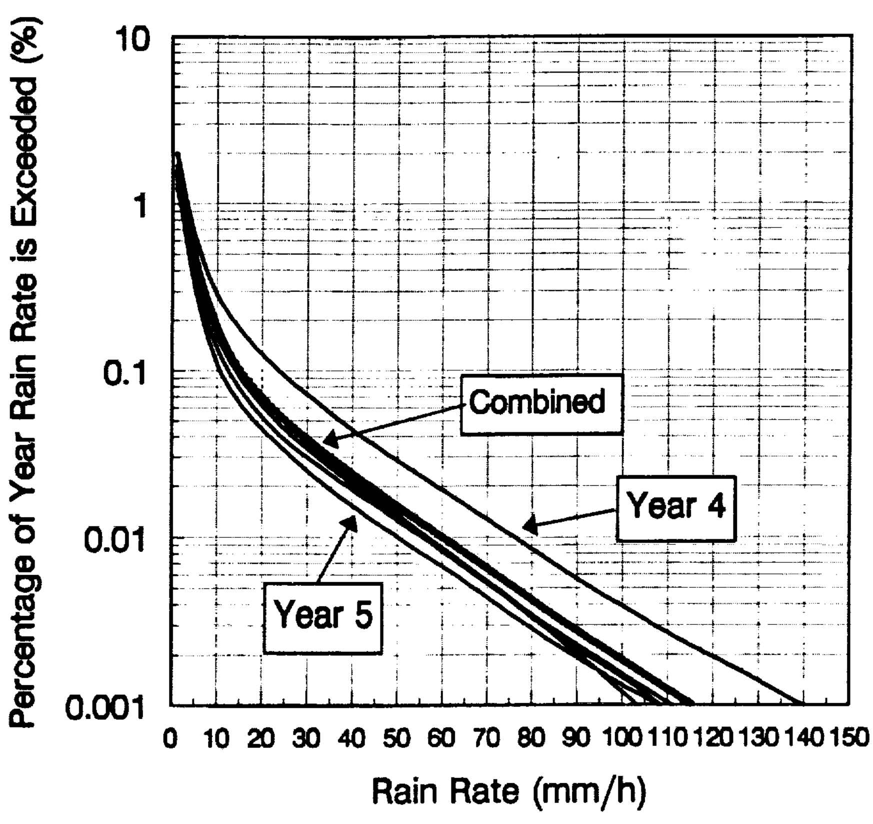

Figure 2: Year-to-year rain rate distributions of network average [1].

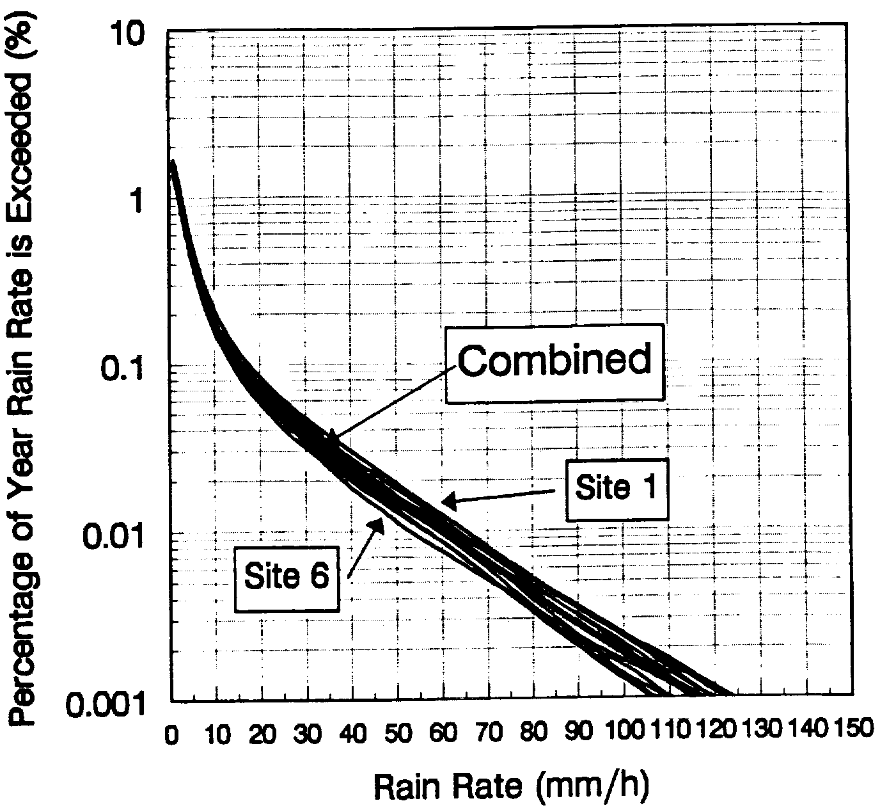

Figure 3: Site-to-site rain rate distributions of five year average [1].

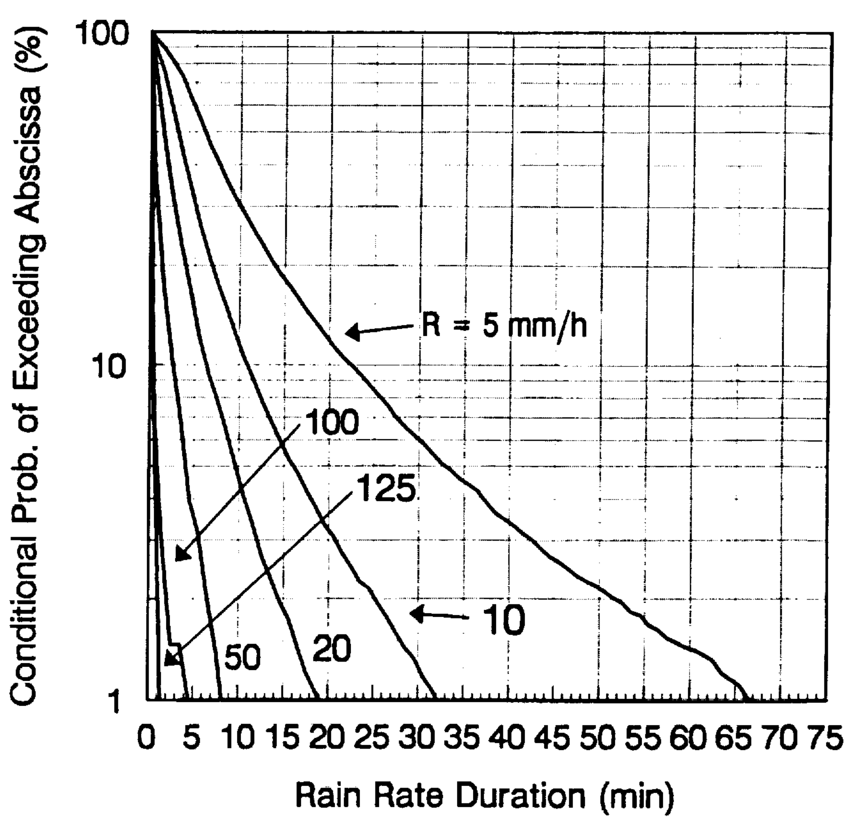

Figure 4: Rain rate duration distributions of combined spatial and temporal average.

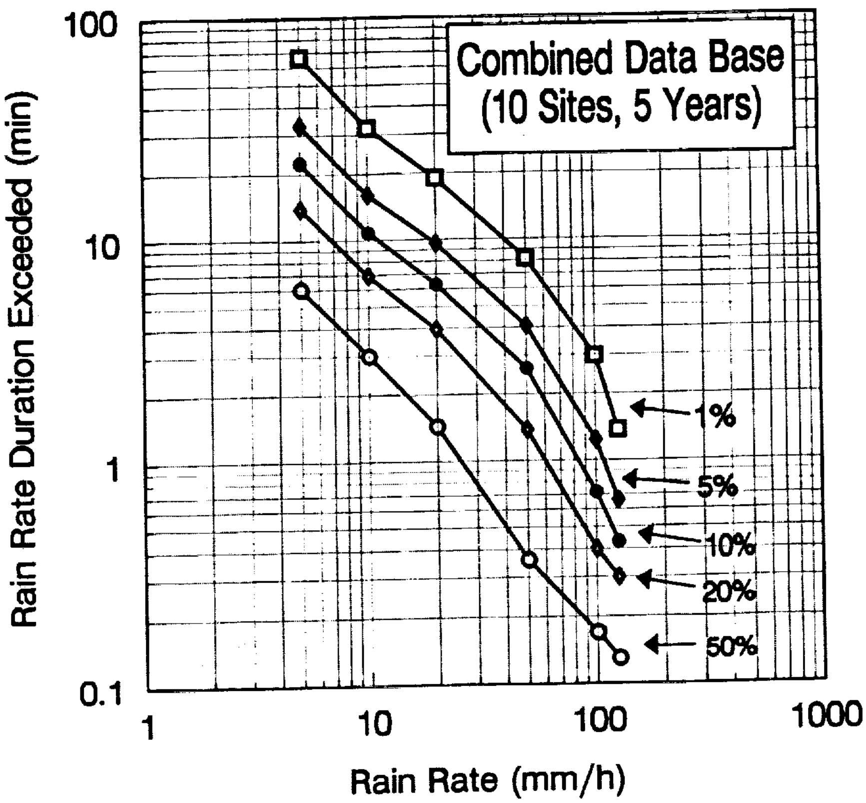

Figure 5: Rain rate duration versus rain rate threshold at equal probability levels.

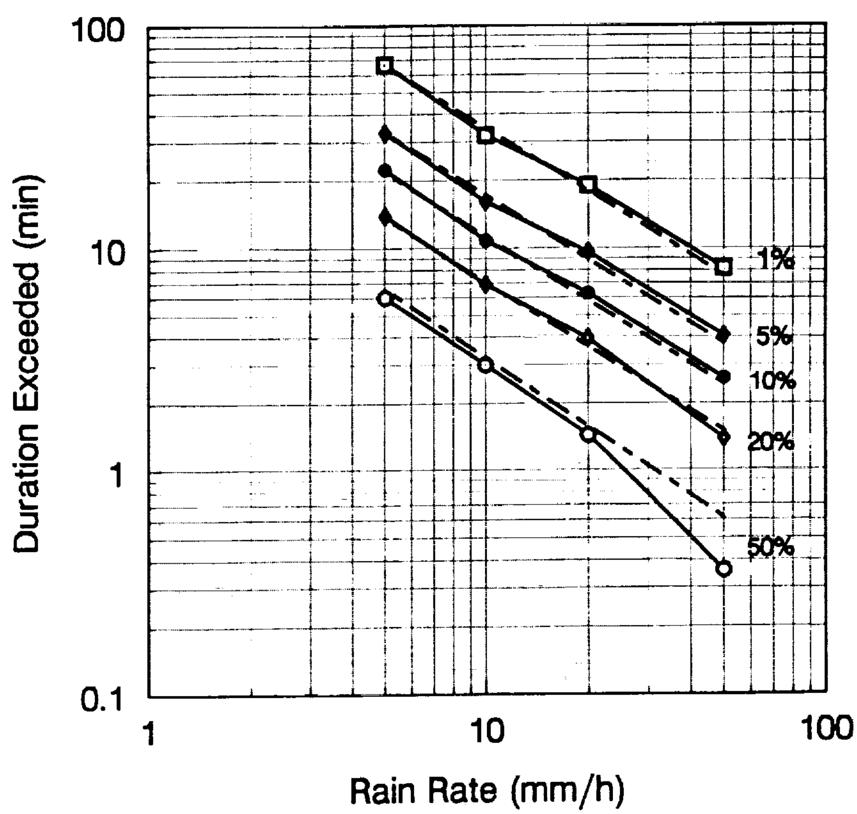

Figure 6: Comparison of measured (solid curve) and empirical model (dashed curve) of rain rate duration versus rain rate threshold at equal probability levels.

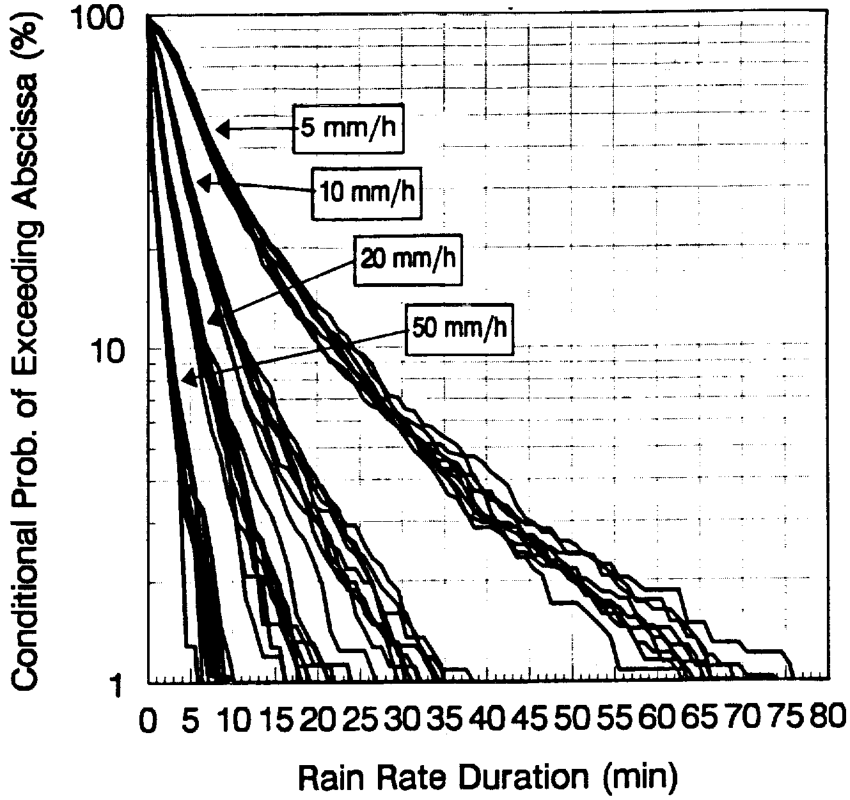

Figure 7: Site-to-site rain rate duration distributions of five year average [1].

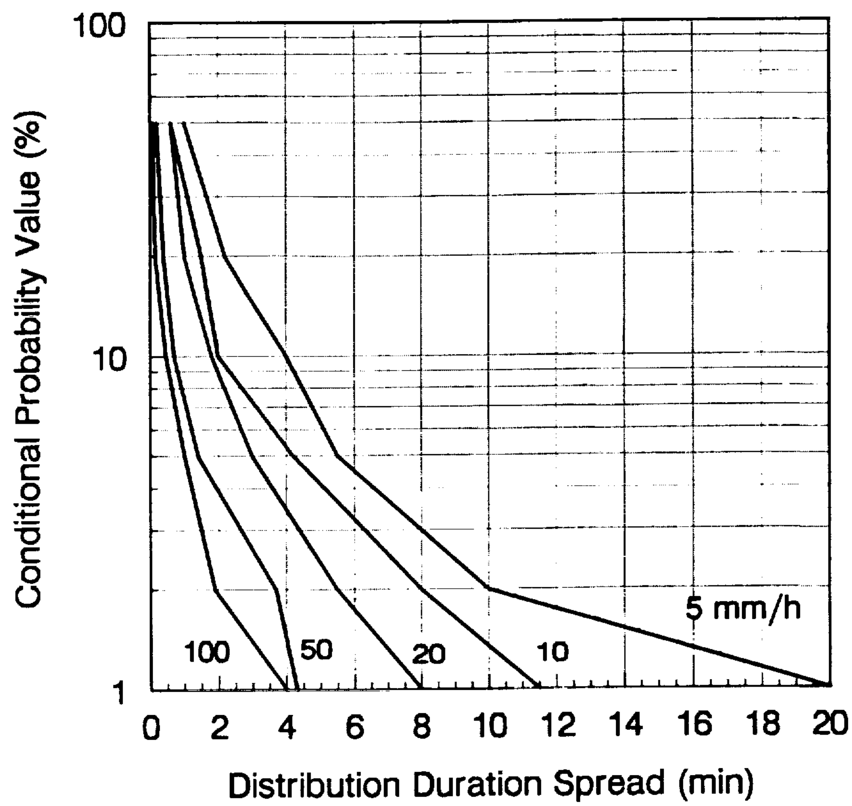

Figure 8: Site-to-site rain rate duration peak spread as a function of probability.

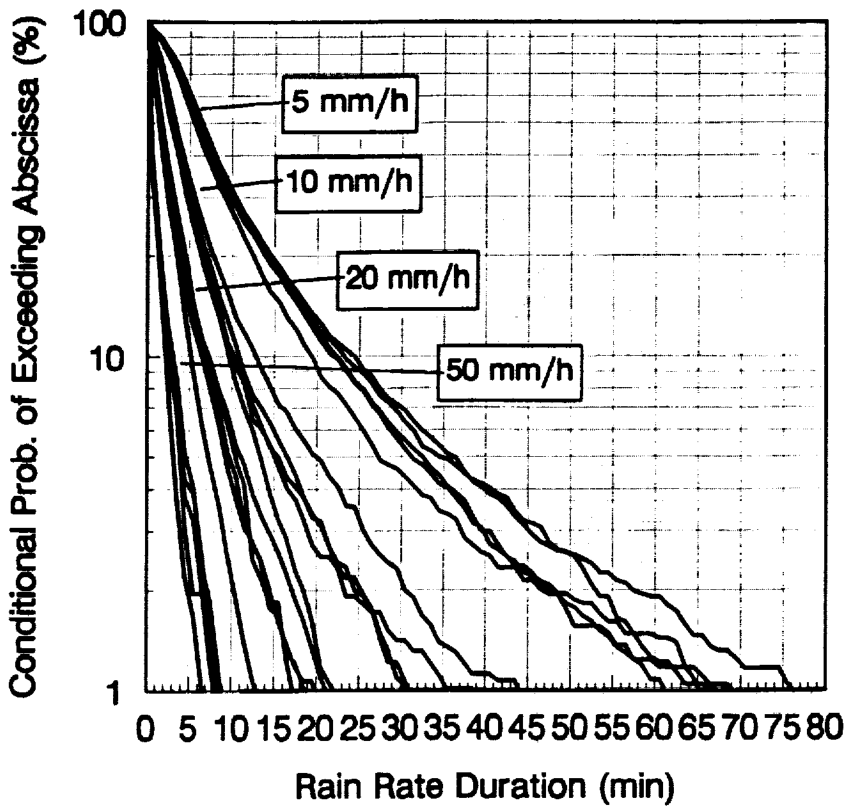

Figure 9: Year-to-year rain rate duration distributions of network average.

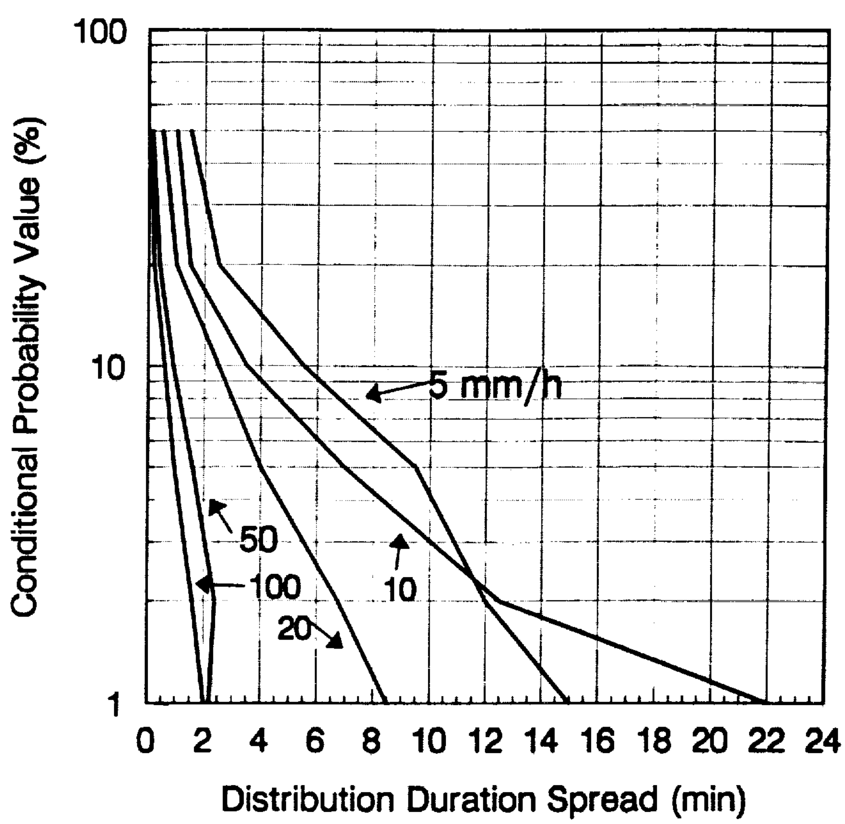

Figure 10: Year-to-year rain rate duration peak spread as a function of probability.

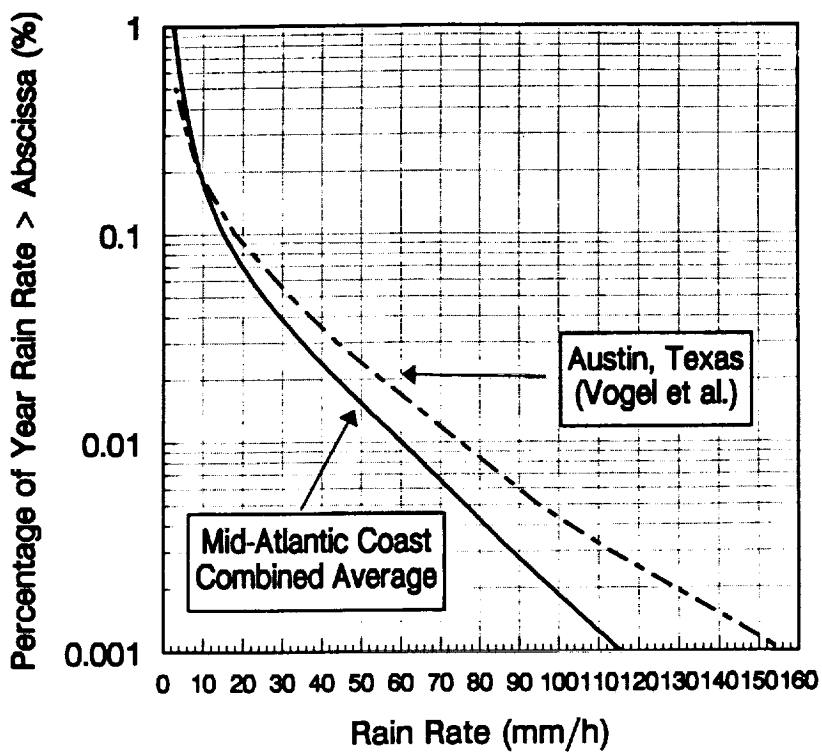

Figure 11: Comparison of cumulative rain rate distributions from Mid-Atlantic coast and Austin, Texas [4].

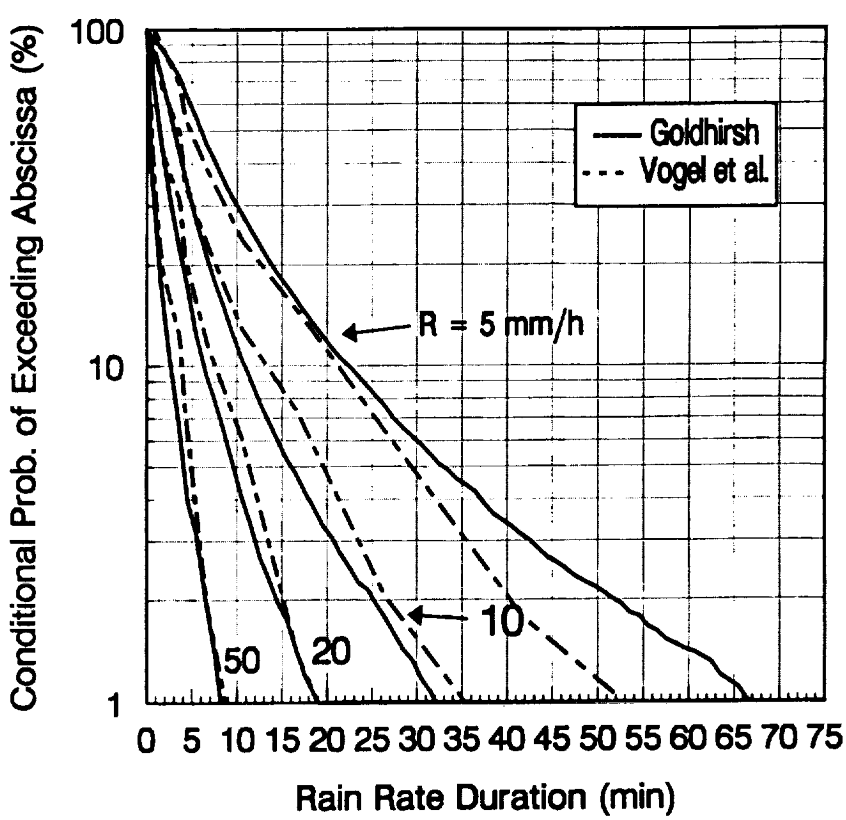

Figure 12: Comparison of cumulative rain rate *duration* distributions from Mid-Atlantic coast and Austin, Texas [4].